JPP Journal of Pharmacy and Pharmacology
ROYAL PHARMACEUTICAL SOCIETY

JPP Journal of Pharmacy and Pharmacology

JPP 2011, 63: 1522–1530

Received October 19, 2010
Accepted August 23, 2011
DOI
10.1111/j.2042-7158.2011.01356.x
ISSN 0022-3573

Research Paper

Hemin-coupled iron(III)-hydroxide nanoparticles show increased uptake in Caco-2 cells

Markus Richard Jahn[a], Ibrahim Shukoor[b], Wolfgang Tremel[b], Uwe Wolfrum[c], Ute Kolb[d], Thomas Nawroth[a] and Peter Langguth[a]

[a]Biopharmacy and Pharmaceutical Technology, Institute of Pharmacy and Biochemistry, [b]Institute of Inorganic and Analytical Chemistry, [c]Cell and Matrix Biology, Institute of Zoology, and [d]Institute of Physical Chemistry, Johannes Gutenberg University, Mainz, Germany

Abstract

Objectives The absorption of commonly used ferrous iron salts from intestinal segments at neutral to slightly alkaline pH is low, mainly because soluble ferrous iron is easily oxidized to poorly soluble ferric iron and ferrous iron but not ferric iron is carried by the divalent metal transporter DMT-1. Moreover, ferrous iron frequently causes gastrointestinal side effects. In iron(III)-hydroxide nanoparticles hundreds of ferric iron atoms are safely packed in nanoscaled cores surrounded by a solubilising carbohydrate shell, yet bioavailability from such particles is insufficient when compared with ferrous salts. To increase their intestinal uptake iron(III)-hydroxide nanoparticles were coupled in this study with the protoporphyrin hemin, which undergoes carrier-mediated uptake in the intestine.

Methods Uptake of iron(III)-hydroxide nanoparticles with hemin covalently coupled by DCC reaction was measured in Caco-2 cells with a colorimetric assay and visualized by transmission electron microscopy.

Key findings Nanoparticles were taken up by carrier-mediated transport, since uptake was temperature-dependent and increased with an increasing hemin substitution grade. Furthermore, uptake decreased with an increasing concentration of free hemin, due to competition for carrier-mediated uptake.

Conclusions Hemin-coupled iron(III)-hydroxide nanoparticles were carried by a heme specific transport system, probably via receptor mediated endocytosis. It can be expected that this system shows improved absorption of iron compared with uncoupled iron(III)-hydroxide nanoparticles, which exist on the market today.

Keywords absorption; Caco-2 cells; iron deficiency; iron(III)-hydroxide nanoparticles; oral delivery

Introduction

Although the therapy of iron deficiency with oral ferrous salts is widely used, the bioavailability of iron from such salts is insufficient.[1] Nutritional components (e.g. phytate in whole grain and bran, oxalic acid in spinach, phosphates in practically all foods or tannins from black tea and coffee) may decrease the absorption of ferrous iron by forming insoluble complexes.[2,3] Also drugs such as tetracyclines, gyrase inhibitors, levodopa, methyldopa and antacids reduce the bioavailability of ferrous iron.[4] The gastrointestinal side effects of ferrous salts as a consequence of oxidative stress are well known.[4,5] In the acidic environment of the stomach ferrous salts are dissolved. Ferrous iron with weakly coordinating anions, such as $FeSO_4$ or ferrous gluconate, represent a source of hydrogenated 'free' ferrous cations, known to cause toxicity.[6] In the Fenton reaction $Fe^{2+} + H_2O_2 \rightarrow Fe^{3+} + {}^{\bullet}OH + OH^-$ ferrous iron reacts with hydrogen peroxide to form hydroxyl radicals. These radicals are highly reactive and oxidise DNA, proteins, carbohydrates and lipids. Ferric iron may become reduced to ferrous iron: $Fe^{3+} + {}^{\bullet}O_2^- \rightarrow Fe^{2+} + O_2$. Catalytic amounts of iron are adequate to generate hydroxyl radicals and to cause oxidative stress: ${}^{\bullet}O_2^- + H_2O_2 \rightarrow {}^{\bullet}OH + HO^- + O_2$ (Haber–Weiss reaction). On the contrary, in the neutral and basic environment of the small intestine soluble ferrous iron is easily oxidized to poorly soluble ferric iron. Therefore uptake via the divalent metal transporter DMT-1, the only transporter for iron molecularly identified so far, is limited.

Correspondence: Peter Langguth, Biopharmacy and Pharmaceutical Technology, Institute of Pharmacy and Biochemistry, Johannes Gutenberg University, Staudingerweg 5, D–55099 Mainz, Germany.
E-mail: langguth@mail.uni-mainz.de

To improve the low tolerability and poor bioavailability of ferrous salts, different approaches have been pursued so far. For example, enteric-coated dosage forms were developed, primarily releasing ferrous iron in the duodenum and therefore resulting in improved gastric tolerability.

Iron(III)-hydroxide nanoparticles (FeONP) are an interesting alternative to ferrous salts. In these formulations hundreds of ferric iron atoms are safely packed into nanoscaled iron(III)-hydroxide cores[7] resulting in less oxidative stress and less side effects while a carbohydrate shell prevents the cores from precipitating. The iron(III)-hydroxide polymaltose complex FeONP_PM (Ferrum Hausmann Sirup, Vifor, München, Germany and Maltofer, Vifor St Gallen, Switzerland), contains an iron(III)-hydroxide core surrounded by a polymaltose shell and has been used in Europe for more than 25 years.[8] Unlike commercially available ferrous salts FeONP_PM is supposed to be absorbed by diffusion through the brush border,[9] is even better absorbed when taken concomitantly with food[10] and interactions of FeONP_PM with a wide range of drugs are held off.[11–13] In a recently published meta-analysis of studies in iron-deficient adults, FeONP_PM was shown to achieve similar haemoglobin levels compared with $FeSO_4$, but was better tolerated.[14]

Nevertheless, doubts remain regarding the bioavailability of FeONP_PM. For example, 14 days after administration in 17 healthy men, 0.81% of the ^{59}Fe-labelled iron dose of FeONP_PM was withheld by the body, compared with 8% of an ^{59}Fe-labelled solution of ferrous ascorbate.[1] Therefore the supposed diffusion of FeONP_PM into enterocytes seems not to be very effective.

In principle, the uptake of nanoparticles via the gastrointestinal mucosa can take place by (i) paracellular passage – as reported for particles <50 nm,[15] if the permeability of the tight junctions is increased by interaction with chitosan[16] or polyacrylic acid;[17] (ii) diffusion into enterocytes – possible for particles <50 nm;[18] (iii) adsorptive endocytosis by enterocytes – possible for particles <500 nm;[15] (iv) receptor-mediated endocytosis by enterocytes – possible for particles coupled with specific ligands;[19–21] and (v) lymphatic uptake by M-cells of the gut-associated lymphoid tissue (GALT), reported for particles <3 μm.[22]

Having these facts in mind, there seems to be at least two approaches to contact FeONP_PM-like nanoparticles with the membrane of enterocytes to enhance their uptake. One is modifying their physicochemical characteristics for (iii) adsorptive endocytosis; in particular charge can enhance adsorption and uptake, probably via electrostatic interaction.[15,23,24] The second approach for enhanced uptake is (iv) modifying the nanoparticles with specific ligands for receptor-mediated endocytosis – this is detailed in the present manuscript, using the example of heme/hemin.

Heme (ferrous protoporphyrin IX) is a ubiquitous organic molecule derived especially from myoglobin in meat and haemoglobin in blood. Heme iron is commonly believed to be the most important source of dietary iron in a typical western diet. A heme iron polypeptide (HIP), allowed for significantly increased iron absorption taken with a meal when compared with ferrous salts.[25]

The uptake of heme is not totally itemized so far and neither a heme receptor nor a heme transporter have been molecularly identified. The gene SLC46A1, which was indentified as a heme carrier protein (HCP-1),[26] is primarily a transporter for folic acid (PCFT, proton-coupled, high-affinity folate transporter).[27] Irrespective of its definitive identity, evidence for a heme transport system exists[28] and seems promising for targeting absorptive transporters.

The aim of this work was to couple FeONP with the specific ligand hemin, which is very similar to heme (protoporphyrin IX containing ferric iron instead of ferrous iron), to target the specific heme transport system on the membrane of enterocytes. The significance of such a system is threefold: (i) targeting by hemin; (ii) iron uptake by hemin containing one iron atom each; and (iii) even more iron uptake by FeONP containing hundreds of iron atoms each.

The uptake in enterocytes of both hemin-coupled and non-coupled FeONP, was studied in Caco-2 cell monolayers, which have enterocyte-like characteristics such as microvilli, tight junctions and duodenal transport systems (e.g. DMT-1[29] or heme transport system[30]). The cell line is also established as an in-vitro model for the uptake of nanoparticles[31] as well as iron salts.[32] Iron uptake was measured by the ferrozine method and visualized by transmission electron microscopy.

Materials and Methods

Chemicals

Dulbecco's modified Eagle's medium (DMEM) containing GlutaMAX I (4.5 g/l D-glucose, without sodium pyruvate), non-essential amino acids (NEAA), penicillin/streptomycin (PEST), trypsin and Hank's buffered salt solution (HBSS) were obtained from Gibco Invitrogen (Karlsruhe, Germany). Fetal bovine serum superior (FBS superior) was purchased from Biochrom (Berlin, Germany). 2-(*N*-Morpholino)-ethanesulfonic acid (MES) was purchased from Roth (Karlsruhe, Germany). Iron(III)-hydroxide dextran complex FeONP_DEX (Cosmofer, 50 mg Fe/ml in 2 ml ampoules; Teva, Mörfelden-Walldorf, Germany) and iron(III)-hydroxide polymaltose complex FeONP_PM (Ferrum Hausmann Sirup, 10 mg Fe/ml in a 200 ml bottle; Vifor, München, Germany) were obtained from a pharmacy. All iron complexes were used immediately after opening the vial or kept at 4°C under nitrogen. Solutions were made from bi-distilled water. For synthesis hemin was purchased from Roth (Karlsruhe, Germany) and 1,6-diaminohexane was purchased from Sigma-Aldrich (Steinheim, Germany). 3-(4,5-Dimethylthiazol-2-yl)-2,5-diphenyltetrazolium bromide (MTT) was obtained from Roth (Karlsruhe, Germany).

Cell culture

Caco-2 cells were purchased from the European Collection of Cell Cultures (ECACC). They were grown in DMEM with GlutaMAX I, 4.5 g/l D-glucose, without sodium pyruvate, supplemented with 10% FBS, 1% non-essential amino acids, 100 U/ml penicillin and 100 μg/ml streptomycin in an atmosphere of 5% CO_2 and 90% relative humidity. For maintenance cells were trypsinized (trypsin–EDTA solution 0.25/0.02%) at 80–90% confluence and medium was replaced every other day. For experiments cells from passages 45–62 were used.

Coupling of FeONP with hemin

Hemin was coupled to FeONP using a method modified from the literature.[33] A reaction scheme is presented in Figure 1. Briefly, the dextran hydroxyl groups in FeONP_DEX (50 mg Fe/ml, 0.9 ml) were oxidized to form aldehyde groups (sodium periodate, 15 mM, 5 ml), followed by dialysis (sodium bicarbonate buffer, MW cut-off 3000, 12 h). To form amine-terminated-tethers, 1,6-diaminohexane (0.2 M, 5 ml) was added to the resulting solution and stirred for 12 h. Afterwards the resulting Schiff's base was reduced (sodium borohydride, 0.07 g/10 ml water–methanol mixture, 12 h) and the mixture was dialysed again (sodium bicarbonate buffer, MW cut-off 3000; 2 × 12 h).

The amine-terminated tethers were coupled with hemin's carboxyl groups to synthesize a low-substituted FeONP_DEX_hemin1 and a high-substituted FeONP_DEX_hemin2. Therefore the carboxyl groups were activated by adding dicylohexylcarbodiimide (DCC, 10 mg for FeONP_DEX_hemin1; 50 mg for FeONP_DEX_hemin2) and *N*-hydroxysuccinimide (NHS, 5 mg; 25 mg) along with triethylamine (TEA, 40 µl; 80 µl) and dimethyl sulfoxide (DMSO, 5 ml; 8 ml) for 24 h in the dark. After removing the by-product dicyclohexylurea by centrifugation, NHS-hemin was reacted with the amine-terminated iron oxide nanoparticle solution to form a covalent bond between nanoparticles and activated ligands (DMSO, 3 h). Finally the mixture was dialysed again (sodium bicarbonate buffer, MW cut-off 3000, 2 × 12 h) and repeatedly ultrafiltrated (MW cut-off 3000, 11 000 g, 30 min) until no hemin was detectable in the filtrate (ultraviolet–visible spectroscopy, see characterization of FeONP).

Structural characterisation of FeONP

Fourier transform infrared spectroscopy

To confirm the synthesized amide bond between hemin and FeONP_DEX, solutions of FeONP_DEX and FeONP_DEX_hemin2 were freeze dried (−56°C, 600 mbar, 36 h; Alpha

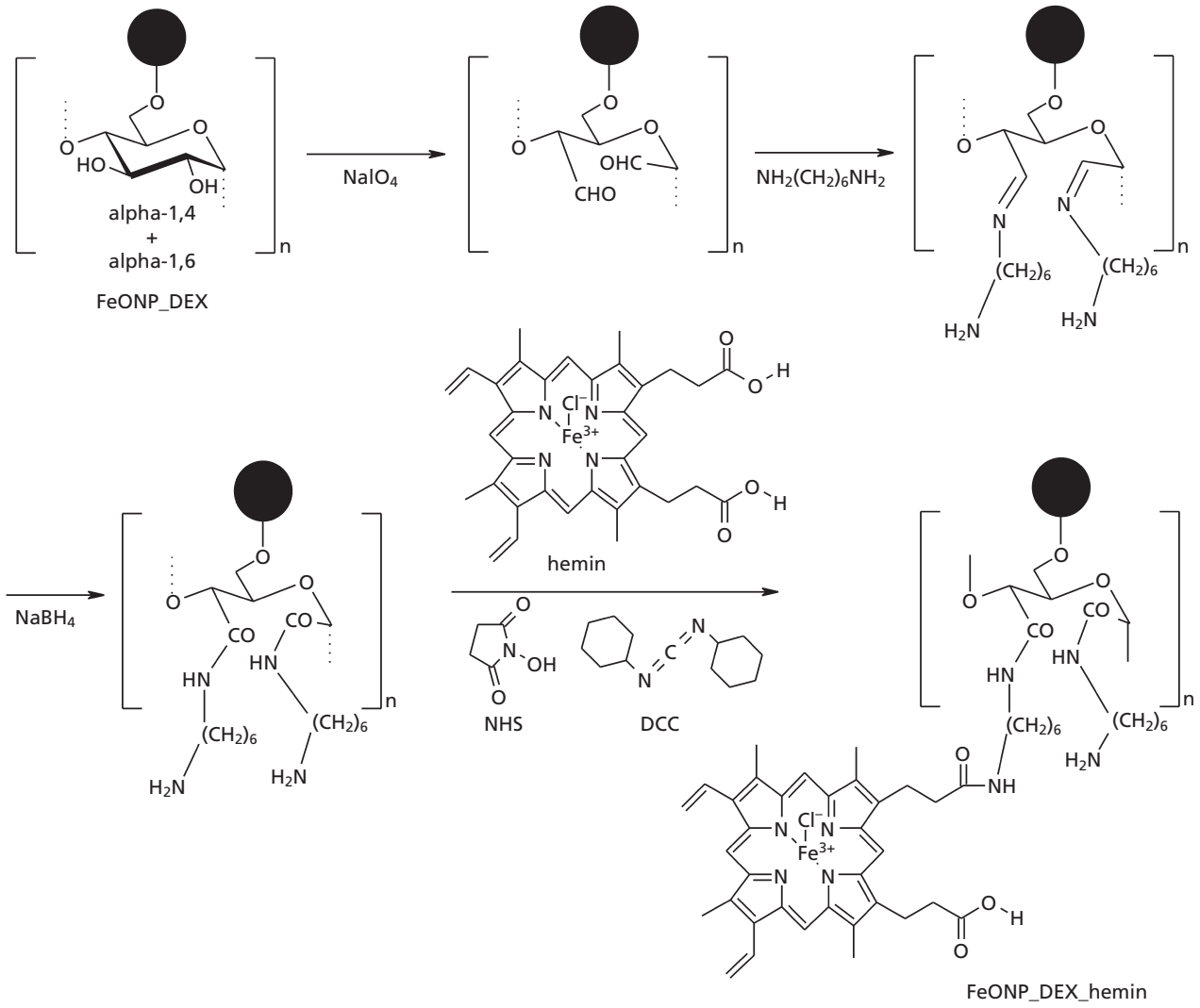

Figure 1 Reaction scheme for the synthesis of FeONP_DEX_hemin. Other reaction paths are possible (e.g. vicinal glucose hydroxyl groups can be oxidised at C3 and C4 instead of C2 and C3). Black circles represent the iron hydroxide core. NHS, *N*-hydroxysuccinimide; DCC, dicyclohexylcarbodiimide.

1–4, Christ, Osterode, Germany) and analysed by Fourier transform infrared spectroscopy (FTIR) (KBr pellet technique; Impact 400 FTIR spectrophotometer + Omnic 1.2 Software; Nicolet Instruments, Warwick, UK).

Ultraviolet–visible spectroscopy

Ultraviolet–visible (UV-VIS) spectra from hemin (0.01 M in 0.1 M NaOH), FeONP_DEX_hemin1 and FeONP_DEX_hemin2 (each 10 μg Fe/ml in 0.1 M NaOH) were taken with a Lambda 20 (Perkin Elmer, Überlingen, Germany). To estimate the molar concentration of hemin in FeONP_DEX_hemin1 and FeONP_DEX_hemin2, a calibration curve with hemin was plotted (0–0.2 mM in 0.1 M NaOH, 387 nm).

Transmission electron microscopy

Using transmission electron microscopy (TIM), the dimension of the iron hydroxide cores was determined with a CM12 transmission electron microscope (FEI/ Philips, Oregon, USA) at 120 kV. All preparations (1 mg Fe/ml) were deposited onto a hydrophilized copper grid (300 mesh, Ø 3 mm) and allowed to dry. The median of the geometrical diameter $d_g = \sqrt{(d_s^2 + d_l^2)/2}$ was determined ($n = 50$, d_s = shortest dimension, d_l = longest dimension).

Dynamic light scattering

The size distribution of the whole particle, which is iron hydroxide core plus carbohydrate shell, was determined by dynamic light scattering (DLS). The diluted samples (0.4 mg Fe/ml) were illuminated by a laser light ($\lambda = 632.8$ nm) and the scattered light was detected by a single photon detection unit that was connected to a correlator (ALV 7004, Langen, Germany) at an angle of 170° with respect to the incident beam. The data was analysed with ALV correlator software 3.0. Intensity distributions were changed into mass distributions.

Quantitative uptake study

Cell-associated iron was quantitatively measured using the ferrozine method.[34] By subtracting the adsorbed iron at 4°C from the sum of adsorbed and incorporated iron at 37°C the active iron uptake into Caco-2 cells was determined.

Briefly, Caco-2 cells grown on 48-well plates for 20–21 days were incubated with solutions of FeONP (200 μg Fe/ml) in HBSS+MES (10 mM) pH 6.5 with or without hemin (0.001 mM and 0.01 mM in 1% DMSO) for 12 h at 4°C and 37°C while being shaken (90 rev/min). After washing four times with ice-cold buffer (3 × HBSS+HEPES (10 mM) pH 7.4 and 1 × HBSS+HEPES (10 mM) + EDTA (1 mM) pH 7.4) 500 μl of 0.01 M HCl were added into each well and mixed with 250 μl of reagent A (4.5% $KMnO_4$ and 1.2 M HCl mixed at equal volumes just before use). Samples were incubated at 60°C for 2 h and allowed to cool to room temperature before adding 50 μl of reagent B (6.5 mM ferrozine, 13.1 mM neocuproine, 2 M ascorbic acid, 5 M ammonium acetate). After 30 min the absorbance of samples was read at 580 nm using a SpectraFluor microplate reader (Tecan, Männedorf, Switzerland). Concentrations were calculated using a standard curve prepared with $FeCl_3$ in 0.01 M HCl, ranging from 0 to 6 μg Fe/ml. Experiments were performed in triplicate.

Qualitative uptake study

To confirm the results on quantitative particle uptake TEM of Caco-2 cells treated with nanoparticles was performed.

Briefly, Caco-2 cells grown on polycarbonate membranes for 20–21 days were incubated with solutions of FeONP (100 μg Fe/ml) in HBSS+MES (10 mM) pH 6.5 for 12 h at 37°C while being shaken (90 rev/min). After washing, cells were pre-fixed with 2.5% glutaraldehyde in 0.1 M cacodylate buffer, pH 7.4 for 1 h, post-fixed with 2% OsO_4 in cacodylate buffer for 1 h at room temperature, dehydrated in a graded series of ethanol (30–100%), infiltrated twice with propylene oxide and once with a 1 : 1 mixture of propylene oxide and araldite resin overnight. For embedding, samples were transferred to pure araldite resin and polymerized for 48 h at 60°C. Ultrathin sections were cut with an Ultracut S diamond knife (Leica, Wetzlar, Germany) and examined with a Technai 12 transmission electron microscope (FEI/ Philips, Oregon, USA) operating at 120 kV.

MTT cytotoxicity assay

In this assay,[35] Caco-2 cells grown on 96-well plates for 20–21 days were incubated with solutions of FeONP (200 μg Fe/ml) in HBSS+MES (10 mM) pH 6.5 for 12 h at 37°C while being shaken (90 rev/min). Cells were washed, incubated with MTT (0.5 mg/ml, 100 μl DMEM/well) for 1 h at 37°C and originating violet crystals were dissolved in 200 μl DMSO and 25 μl glycine buffer (0.1 M glycine, 0.1 M NaCl, pH 10.5). After 30 min, the absorption was read at 580 nm using a SpectraFluor microplate reader (Tecan, Männedorf, Switzerland). Untreated cells were set at 100% viable. Experiments were performed in triplicate

Statistical methods

For statistical analysis of the quantitative uptake mean values of absorption at 4°C were subtracted from mean values of absorption at 37°C. Differences between iron uptake values were compared using the Kruskal–Wallis rank sum test (S-Plus, MathSoft Inc.) applying a two-sided alternative to the null hypothesis. $P \leq 0.05$ was considered as significant. Pairwise comparison was performed using the Wilcoxon rank test.

Results

Coupling of hemin with nanoparticles

FTIR-spectra of FeONP_DEX, FeONP_DEX_hemin2 and hemin are shown in Figure 2. Hemin absorption between 1620 and 1720 cm^{-1} is related to C = O stretching modes of carboxyl groups in hemin. In the spectrum of FeONP_DEX_hemin2 the C = O stretching vibration of hemin is shifted bathochromically to 1520–1620 cm^{-1}. This indicates that hemin's carboxyl groups reacted with the linker's amino groups to an amide and therefore that hemin was coupled with FeONP_DEX. For explanation of the other bands see Alben[36] and Figure 2.

To estimate the degree of hemin substitution in FeONP_DEX_hemin UV-VIS studies were carried out. In Figure 3 FeONP_DEX_hemin2 clearly shows hemin absorption bands at 350 nm and 387 nm whereas FeONP_DEX_hemin1 only

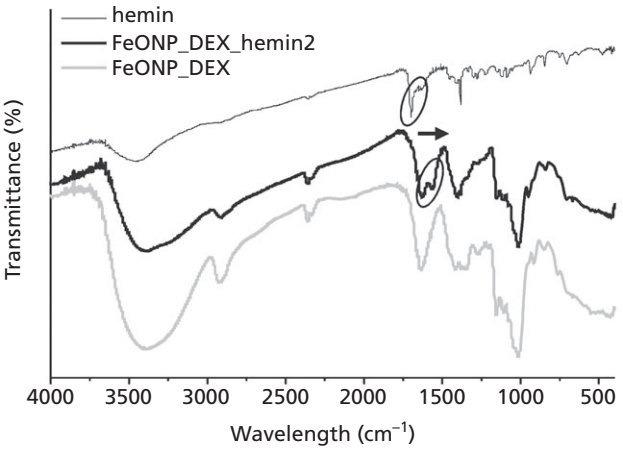

Figure 2 Fourier transform infrared spectra of FeONP_DEX, FeONP_DEX_hemin2 and hemin and bathochromic shift of the hemin C = O stretching mode after coupling with FeONP_DEX. Bands at about 3400 cm^{-1} (wide) and 1600 cm^{-1} result from O-H stretching and O-H deformation vibrations in dextran or adsorbed water. Dextran C-H stretching and deformation modes are identified at about 2900 cm^{-1} and 1100–1450 cm^{-1}. Bands in the range of 1000–1150 cm^{-1} are dextran C-O stretching modes. Hemin absorption at about 1380 cm^{-1} is a C-H deformation mode of -CH_3 in the pyrrol ring. The bathochromic shift of hemin's C = O stretching mode in the free substance (1620 and 1720 cm^{-1}, carboxyl) and in FeONP_DEX-hemin2 (1520 and 1620 cm^{-1}, amide) is marked. Characteristic bands for iron hydroxide in the range of 400–1000 cm^{-1} are probably overlapped by the dextran finger print.

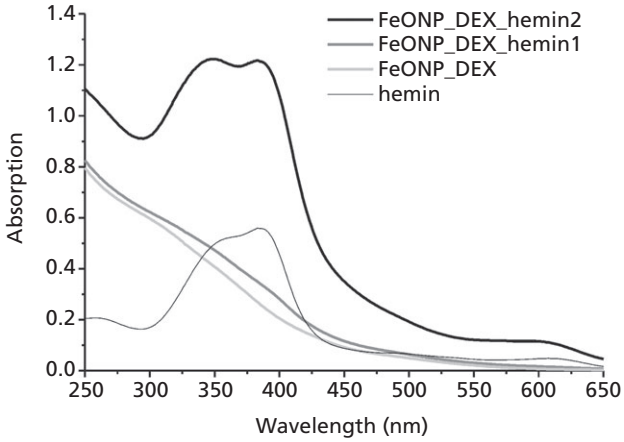

Figure 3 Comparison of the UV-VIS spectra of hemin, FeONP_DEX, low-substituted FeONP_DEX_hemin1 and high-substituted FeONP_DEX_hemin2 at 387 nm. Concentrations: hemin 0.01 mM, FeONP 10 μg Fe/ml.

shows a slightly increased absorption compared with FeONP_DEX. From the hemin calibration curve the molecular hemin concentration in FeONP_DEX_hemin was determined (1.5 μM hemin in FeONP_DEX_hemin1, 18.2 μM hemin in FeONP_DEX_hemin2, each 10 μg Fe/ml). With the mass concentration c_{FeONP_DEX} = 312.5 mg/ml[37] (undiluted solution, 50 mg Fe/ml) and the molecular weight M_{FeONP_DEX} = 165 000 g/mol[38] the molecular nanoparticle concentration c_{FeONP_DEX} = 312.5 mg/ml/165 000 g/mol = 1.89 mM was calculated, which equates to 0.379 μM in the diluted 10 μg Fe/ml sample. Therefore there are about 1.5 μM/0.379 μM = 4 molecules hemin per nanoparticle in FeONP_DEX_hemin1 and 18.2 μM/0.379 μM = 48 molecules hemin per nanoparticle in FeONP_DEX_hemin2. A physical mixture can be excluded as all unbound hemin was ultracentrifugated and abolished.

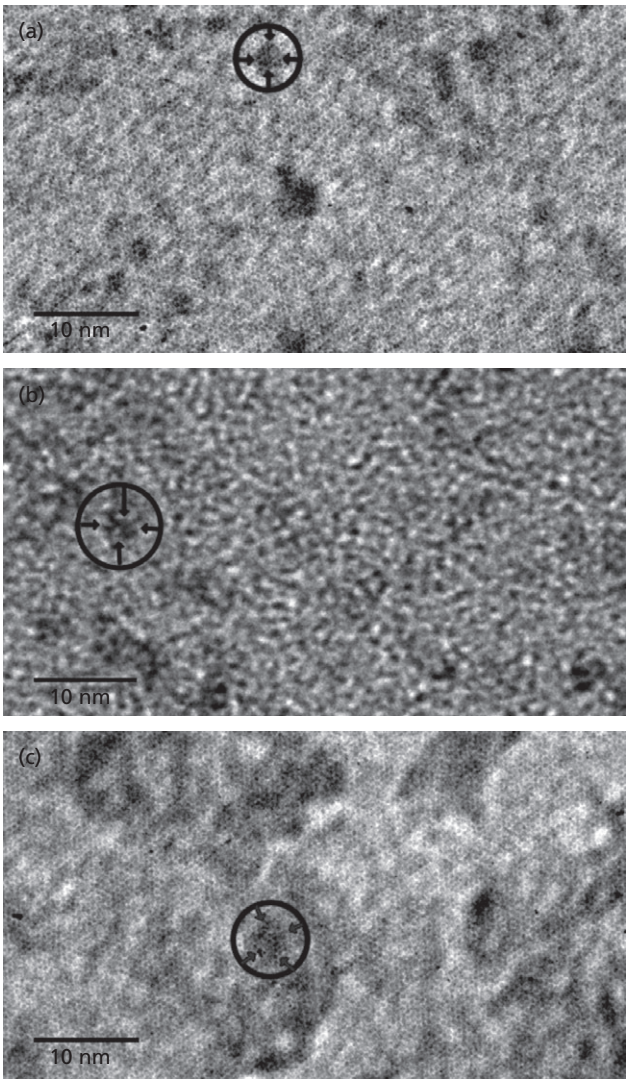

Figure 4 Transmission electron microscopy images of FeONP_PM (a), FeONP_DEX (b) and FeONP_DEX _hemin2 (c). The particle measurement is exemplified by a circle with arrows.

Size of core and whole particle

TEM images of FeONP_PM, FeONP_DEX and FeONP_DEX_hemin2 are shown in Figure 4. Dark, electron dense, beadlike structures represent the iron hydroxide cores, surrounded by a less electron dense matrix, which can be attributed to the carbohydrate fraction. Measurement of the geometrical diameter was used to estimate the size of the cores, which was 2.5 ± 0.6 nm (1.3–4.1 nm) for FeONP_PM, 4.9 ± 1.0 nm (2.8–7.0 nm) for FeONP_DEX and 4.5 ± 1.3 nm (2.2–7.7 nm) for FeONP_DEX_hemin2. Obviously, the size of cores did not change during coupling with hemin.

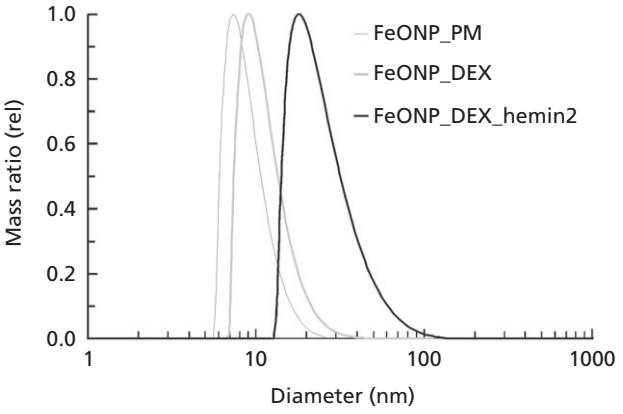

Figure 5 Mass distribution of the hydrodynamic diameter of FeONP_PM, FeONP_DEX and FeONP_DEX _hemin2.

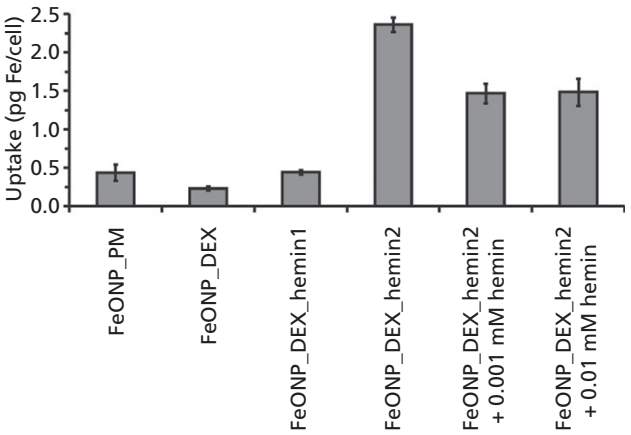

Figure 6 Cell-associated iron of FeONP_PM, FeONP_DEX, hemin-coupled FeONP_DEX_hemin1 (low substituted) and FeONP_DEX_hemin2 (high substituted) in Caco-2 cells. Active uptake is represented by difference between cell-associated iron at 37°C and 4°C. Uptake of FeONP_DEX_hemin2 is competitively inhibited by free hemin. Conditions: 200 µg Fe/ml, 12 h, pH 6.5. Data are represented as mean ± SD with $n = 3$. On the basis of the Kruskal–Wallis rank sum test, the null hypothesis of equal uptake between different particles was rejected at $P \leq 0.05$. Multiple comparisons resulted in the following significant differences: FeONP_DEX_hemin2 greater than all other particle uptakes; FeONP_DEX_hemin2+0.001 mM hemin greater than FeONP_DEX_hemin1, FeONP_DEX, FeONP_PM; FeONP_DEX_hemin2+0.01 mM hemin greater than FeONP_DEX_hemin1, FeONP_DEX, FeONP_PM; FeONP_DEX_hemin1 greater than FeONP_DEX.

As also seen in Figure 4, cores tended to cluster. X-ray measurements (data not shown) revealed particle sizes in the same range as above and suggest that clustered cores did not form a continuous phase. Therefore clustering seems not to be representative in solution and is rather because solvent is evaporated during TEM preparation.

The hydrodynamic diameter determined with DLS also measures the carbohydrate shell of the FeONP. In In Figure 5 narrow mass distributions of the particle diameters are shown. At 0.4 mg Fe/ml the median diameters were 9 nm ± 10% for FeONP_PM, 12 nm ± 10% for FeONP_DEX and 29 nm ± 10% for FeONP_DEX-hemin2, indicating, that the particle shell slightly grew after coupling with hemin.

Uptake of FeONP_PM, FeONP_DEX and FeONP_DEX_hemin

To investigate the role of a putative hemin transporter HCP-1/PCFT or a putative hemin receptor (see Discussion) on the internalization of nanoparticles in enterocyte-like Caco-2 cells, the uptake of FeONP_DEX_hemin in comparison with FeONP_DEX was investigated. Therefore, the FeONP were incubated at 4°C and 37°C for 12 h at a concentration of 200 µg Fe/ml. In Figure 6 the iron uptake (pg Fe/cell) is shown, which is the difference between the cell-associated iron at 37°C (adsorption and energy dependent uptake) and 4°C (only adsorption). With an increasing hemin substitution grade the iron uptake, and therefore the nanoparticle uptake, increased (see Figure 6). After incubation with FeONP_DEX-_hemin2, with about 48 hemin molecules in the shell, the iron uptake was 10-times higher compared with the control FeONP_DEX (2.36 ± 0.10 pg Fe/cell vs 0.23 ± 0.02 pg Fe/cell). Accordingly with FeONP_DEX_hemin1, with only four hemin molecules in the shell, iron uptake was lower (0.44 ± 0.03 pg Fe/cell), and about twice as high compared with the control. To check whether there is a specific binding of the nanoparticle via coupled hemin, the higher substituted FeONP_DEX_hemin2 was incubated together with an increasing concentration of dissolved hemin (see Figure 6). At concentrations of 0.001 mM and 0.01 mM hemin the iron uptake decreased by the factor 0.6. However, a 50% inhibition of the uptake was not achieved and iron uptake into the cells again increased at higher concentrations of hemin (data not shown; for possible explanation see Discussion). The uptake of FeONP_PM was low (0.43 ± 0.11 pg/cell), similar to FeONP_DEX.

In Figure 7 representative Caco-2 cells are shown, which were incubated with FeONP (100 µg Fe/ml, 12 h, pH 6.5). The TEM images strongly support the results of the quantitative uptake. After incubation with FeONP_PM and FeONP_DEX no adsorption or uptake of iron hydroxide cores was observable (see Figure 7a and 7b). In contrast, after incubation with FeONP_DEX_hemin2 iron hydroxide cores adhered on the cell membrane and were absorbed by endocytic vesicles (see Figure 7c).

None of the FeONP showed any toxicity in the MTT assay when compared with control without FeONP (data not shown).

Discussion

In principle there are two different strategies to achieve an interaction of nanoparticles with enterocytes or M-cells: (i) by non-specific adsorption (e.g. by electrostatic attraction); or (ii) by specific binding to receptors and ligands. In this work the latter technique was evaluated.

On the surface of enterocytes and M-cells, cell-specific carbohydrates and receptors are localized. Nanoparticles loaded with lectins and specific ligands selectively bind to these structures. For example, it was shown that the oral uptake of tomato lectin-coupled nanoparticles was increased

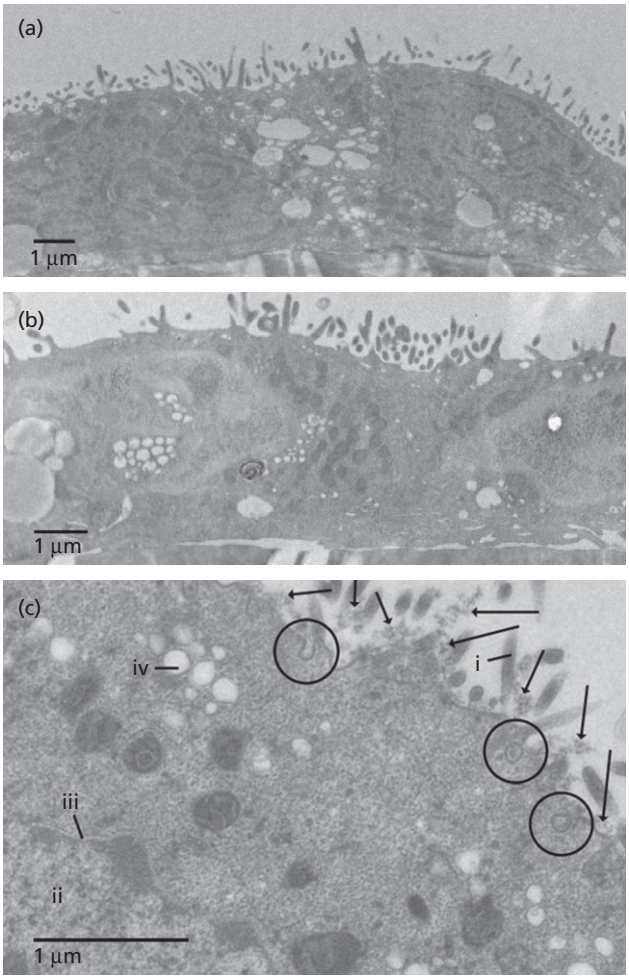

Figure 7 Transmission electron microscopy images of Caco-2 cells after incubation with FeONP_PM (a), FeONP_DEX (b) and FeONP_DEX _hemin2 (c). Arrows tag iron hydroxide cores, circles enclose endocytosis events. (i) Microvilli; (ii) cell core; (iii) core membrane; (iv) lipid droplet. Conditions: 100 μg Fe/ml, 12 h, pH 6.5.

in rats and mainly occurs via normal enterocytes and not via the GALT.[19] Vitamin B_{12} bound to nanoparticles allowed their transport from the apical to basolateral side of Caco-2 cells.[20] The system was used as a carrier for oral delivery of insulin.[21]

A transport mechanism that is potentially exclusive for iron, that is more effective than DMT-1 and that allows the transport of large molecules, ideally nanoparticles, would be useful. The heme receptor or heme transporter thus seems to be very interesting. Bioavailability of heme iron is higher compared with non-heme iron, which argues for the efficiency of a heme transport system.[28] Receptor-mediated endocytosis could be used to introduce several hundreds of iron atoms with one hemin-coupled FeONP. Keeping in mind that with each molecule of hemin just one iron atom is transported, hemin-coupled FeONP should be more effective. Free hemin in the circulation is considered to be toxic, based on observations of severe haemolysis or myolysis as a consequence of diseases such as sickle cell disease, ischaemia reperfusion, and malaria, resulting in high levels of free hemin.[39]

It is expected, however, that the doses of hemin administered together with the FeONP will remain low and will not result in severe increases of free hemin in the circulation. It should also be noted that hemopexin binds hemin with high affinity and scavenges the heme absorbed or released and thus protects the body from the potentially toxic effects of free hemin. In this cascade of events, the hemopexin–hemin complex is taken up by the liver in a saturable, time-dependent, energy-dependent and temperature-dependent process, resulting in the accumulation of heme in the hepatocytes while the hemopexin is released intact.[40]

However, so far neither a heme receptor nor a heme transporter has been identified on a molecular level. The hypothesis of a receptor-mediated endocytosis has its origin in 1979 with the discovery of a heme-binding protein in the pig and human duodenal brush-border membrane.[41] Several studies followed, which demonstrated the existence of a heme binding protein on the surface of enterocytes, hepatocytes and erythroleukaemia cells.[42–44] Also it was shown that heme is taken up into enterocytes as an intact molecule and that subsequently heme is present in endocytic vesicles in the cytoplasm.[45,46] Recently a protein was identified as the intestinal heme transporter HCP-1 (heme carrier protein)[26] and also verified in Caco-2 cells;[30] follow-up studies, however, have shown that the primary function of the protein is a high-affinity proton-coupled transport of folate (proton-coupled folate transporter, PCFT).[27]

Despite the open questions regarding the molecular mechanism of heme uptake there is evidence for an efficient heme transport system, irrespective of its nature. Thus, the uptake of heme is actively regulated in the small intestine, which was demonstrated by increased mucosal uptake in iron-deficient rats compared with fully replete rats.[47] Caco-2 cell studies have shown that the uptake of heme[30] and heme-like zinc protoporphyrin[48] is saturable and temperature dependent and that hemin (i.e. oxidized heme) is actively absorbed and secreted.[49]

In this work FeONP_DEX_hemin1 coupled with an average of four molecules of hemin per nanoparticle was absorbed 1.8 times more than control FeONP_DEX (see Figure 6). FeONP_DEX_hemin2 coupled with an average of 48 hemin molecules was absorbed 10 times more than FeONP_DEX. TEM images visualize FeONP_DEX_hemin2 and not FeONP_DEX being absorbed by endocytic vesicles (see Figure 7b and 7c). At the same time iron uptake by FeONP_DEX_hemin2 was competitively inhibited by 0.001 mM hemin (0.06 μg Fe/ml) and 0.01 mM hemin (0.56 μg Fe/ml) by a factor of 0.6 (see Figure 6). Therefore, altogether it was shown that the uptake of particles resulted from the hemin coupled to the surface of the FeONP and was carried out by a specific hemin/heme receptor or transporter, as demonstrated by temperature dependence, concentration dependence and inhibition by free hemin.

The high uptake capacity of FeONP_DEX_hemin2 (2.36 ± 0.10 pg Fe/cell) is in the same range as observed for the receptor-mediated endocytosis of folic acid coupled FeONP (1.5 pg iron/cell, HeLa cells, 4 h).[50] In contrast the uptake capacity of FeONP_DEX and FeONP_PM is

comparatively low and results from a different uptake mechanism. For FeONP_PM diffusion across the mucosal barrier was suggested.[9] This is in accordance with TEM images in Figure 7, showing no endocytic vesicles in the case of FeONP_PM. As FeONP_PM and FeONP_DEX both have neutral hydrophilic shells, the same uptake mechanism can be assumed.

In the body it remains unclear, whether FeONP-uptake by enterocytes or M-cells is advantageous. FeONP could be taken up into hepatic portal vein via the intestine[51] but also into venous circulation via the gut-associated lymphoid tissue (GALT).[51] Even more likely, FeONP may become lysosomally degraded in enterocytes and originating ionic iron may be transported to blood by basolateral ferroportin, which is the physiological absorptive pathway for ionic iron. In this case a quick degradation of iron(III)-hydroxide cores is essential, keeping in mind that enterocytes are scaled off every third to fifth day.

Coupling of hemin is not restricted to FeONP, it also could be the carrier of other nanoparticles. Therefore hemin-coupled nanoparticles loaded with other active agents like proteins could be utilised to achieve higher bioavailability of these drugs, similar to vitamin B_{12}-coupled nanoparticles.[21]

Conclusions

Intestinal FeONP uptake may be increased up to 10 times with an increasing hemin substitution grade and decreased with an increasing concentration of free and competitive hemin. Therefore hemin-coupled FeONP are transported by a hemin/heme specific transport system. TEM images provide further evidence that hemin-coupled FeONP are taken up by receptor-mediated endocytosis, whereas uncoupled FeONP appeared to diffuse across the membrane. Regarding the oral therapy of iron deficiency our studies present a first step to reach the goal of better absorption of iron via hemin-coupled FeONP as compared with uncoupled FeONP (e.g. Ferrum Hausmann Sirup, which has been on the German market for more than 25 years). Regarding the oral therapy of diseases other than iron deficiency the protoporphyrine hemin might present an adequate ligand of other drug-loaded nanoparticles as well.

Declarations

Conflict of interest

The Author(s) declare(s) that they have no conflicts of interest to disclose.

Funding

This research received no specific grant from any funding agency in the public, commercial, or not-for-profit sectors.

Acknowledgements

Elisabeth Sehn and Rudolf Würfel are greatly acknowledged for their assistance with TEM preparations and analysis. Sören Fütterer is greatly acknowledged for general assistance.

References

1. Heinrich HC. [Bioavailability and therapeutic efficacy of oral iron(II)- and iron(III) preparations]. *Dtsch Apoth Ztg* 1986; 126: 681–690 [in German].
2. Gillooly M *et al*. The effects of organic acids, phytates and polyphenols on the absorption of iron from vegetables. *Br J Nutr* 2007; 49: 331–342.
3. Hallberg L. Bioavailability of dietary iron in man. *Annu Rev Nutr* 1981; 1: 123–147.
4. Ammon HPT. *[Drug Side Effects and Drug Interactions]*, 1st edn. Stuttgart: Wissenschaftliche Verlagsgesellschaft, 2001 [in German].
5. Geisser P. Iron therapy and oxidative stress. *Met Based Drugs* 1997; 4: 137–152.
6. Halliwell B, Gutteridge JM. Role of free radicals and catalytic metal ions in human disease: an overview. *Methods Enzymol* 1990; 186: 1–85.
7. Jahn MR *et al*. CE characterization of potential toxic labile iron in colloidal parenteral iron formulations using off-capillary and on-capillary complexation with EDTA. *Electrophoresis* 2007; 28: 2424–2429.
8. Geisser P. Safety and efficacy of iron (III)-hydroxide polymaltose complex: a review of over 25 years experience. *Arzneimittelforschung* 2007; 57: 439–452.
9. Geisser P, Muller A. Pharmacokinetics of iron salts and ferric hydroxide-carbohydrate complexes. *Arzneimittelforschung* 1987; 37: 100–104.
10. Lundqvist H, Sjöberg F. Food interaction of oral uptake of iron: a clinical trial using ^{59}Fe. *Arzneimittelforschung* 2007; 57: 401–416.
11. Burckhardt-Herold S *et al*. Interactions between iron (III)-hydroxide polymaltose complex and commonly used drugs: simulations and in vitro studies. *Arzneimittelforschung* 2007; 57: 360–369.
12. Potgieter MA *et al*. Effect of an oral iron(III)-hydroxide polymaltose complex on tetracycline pharmacokinetics in patients with iron deficiency anemia. *Arzneimittelforschung* 2007; 57: 385–391.
13. Potgieter MA *et al*. Effect of oral aluminium hydroxide on iron absorption from iron(III)-hydroxide polymaltose complex in patients with iron deficiency anemia: a single-centre randomized controlled isotope study. *Arzneimittelforschung* 2007; 57: 392–400.
14. Toblli JE, Brignoli R. Iron(III)-hydroxide polymaltose complex in iron deficiency anemia: review and meta-analysis. *Arzneimittelforschung* 2007; 57: 431–438.
15. Jung T *et al*. Biodegradable nanoparticles for oral delivery of peptides: is there a role for polymers to affect mucosal uptake? *Eur J Pharm Biopharm* 2000; 50: 147–160.
16. Schipper NG *et al*. Chitosans as absorption enhancers for poorly absorbable drugs 2: mechanism of absorption enhancement. *Pharm Res* 1997; 14: 923–929.
17. Kriwet B, Kissel T. Poly (acrylic acid) microparticles widen the intercellular spaces of caco-2 cell monolayers: an examination by confocal laser scanning microscopy. *Eur J Pharm Biopharm* 1996; 42: 233–240.
18. Sun C *et al*. Magnetic nanoparticles in mr imaging and drug delivery. *Adv Drug Deliv Rev* 2008; 60: 1252–1265.
19. Hussain N *et al*. Enhanced oral uptake of tomato lectin-conjugated nanoparticles in the rat. *Pharm Res* 1997; 14: 613–618.
20. Russell-Jones GJ *et al*. Vitamin B12-mediated transport of nanoparticles across caco-2 cells. *Int J Pharm* 1999; 179: 247–255.

21. Chalasani KB *et al*. A novel vitamin B12-nanosphere conjugate carrier system for peroral delivery of insulin. *J Control Release* 2007; 117: 421–429.
22. Jani P *et al*. Nanoparticle uptake by the rat gastrointestinal mucosa: quantitation and particle size dependency. *J Pharm Pharmacol* 1990; 42: 821–826.
23. Behrens I *et al*. Comparative uptake studies of bioadhesive and non-bioadhesive nanoparticles in human intestinal cell lines and rats: the effect of mucus on particle adsorption and transport. *Pharm Res* 2002; 19: 1185–1193.
24. Pinto-Alphandary H *et al*. Visualization of insulin-loaded nanocapsules: in vitro and in vivo studies after oral administration to rats. *Pharm Res* 2003; 20: 1071–1084.
25. Seligman PA *et al*. Clinical studies of hip: an oral heme-iron product. *Nutr Res* 2000; 20: 1279–1286.
26. Shayeghi M *et al*. Identification of an intestinal heme transporter. *Cell* 2005; 122: 789–801.
27. Qiu A *et al*. Identification of an intestinal folate transporter and the molecular basis for hereditary folate malabsorption. *Cell* 2006; 127: 917–928.
28. West AR, Oates PS. Mechanisms of heme iron absorption: current questions and controversies. *World J Gastroenterol* 2008; 14: 4101–4110.
29. Tandy S *et al*. NRAMP2 expression is associated with ph-dependent iron uptake across the apical membrane of human intestinal caco-2 cells. *J Biol Chem* 2000; 275: 1023–1029.
30. Latunde-Dada GO *et al*. Haem carrier protein 1 (HCP1): expression and functional studies in cultured cells. *FEBS Lett* 2006; 580: 6865–6870.
31. Desai MP *et al*. The mechanism of uptake of biodegradable microparticles in caco-2 cells is size dependent. *Pharm Res* 1997; 14: 1568–1573.
32. Alvarez-Hernandez X *et al*. Caco-2 cell line: a system for studying intestinal iron transport across epithelial cell monolayers. *Biochim Biophys Acta* 1991; 1070: 205–208.
33. Choi H *et al*. Iron oxide nanoparticles as magnetic resonance contrast agent for tumor imaging via folate receptor-targeted delivery. *Acad Radiol* 2004; 11: 996–1004.
34. Fish WW. Rapid colorimetric micromethod for the quantitation of complexed iron in biological samples. *Methods Enzymol* 1988; 158: 357–364.
35. National Cancer Institute. NCL method GTA-1, version 1.0, LLC-PK1 kidney cytotoxicity assay. 2005.
36. Alben JO. Infrared spectroscopy of porphyrins. In: Dolphin D, ed. *The Porphyrins, Volume III, Physical Chemistry, Part A*. New York: Academic Press, 1978: 323–345.
37. Teva Germany. Cosmofer® summary of product characteristics. 2007.
38. Watson Pharma. Infed® iron dextran injection USP. 2006.
39. Kumar S, Bandyopadhyoy U. Free heme toxicity and its detoxification system in humans. *Toxicol Lett* 2005; 157: 175–188.
40. Smith A, Morgan WT. Hemopexin-mediated heme uptake by liver. Characterization of the interaction of heme-hemopexin with isolated rabbit liver plasma membranes. *J Biol Chem* 1984; 259: 12049–12053.
41. Gräsbeck R *et al*. An intestinal receptor for heme. *Scand J Haematol* 1979; 23: 5.
42. Galbraith RA. Heme binding to HEPG2 human hepatoma cells. *J Hepatol* 1990; 10: 305–310.
43. Galbraith RA *et al*. Heme binding to murine erythroleukemia cells. Evidence for a heme receptor. *J Biol Chem* 1985; 260: 12198–12202.
44. Gräsbeck R *et al*. Spectral and other studies on the intestinal haem receptor of the pig. *Biochim Biophys Acta* 1982; 700: 137–142.
45. Parmley RT *et al*. Ultrastructural cytochemistry and radioautography of hemoglobin–iron absorption. *Exp Mol Pathol* 1981; 34: 131–144.
46. Yin Win K, Feng S-S. Effects of particle size and surface coating on cellular uptake of polymeric nanoparticles for oral delivery of anticancer drugs. *Biomaterials* 2005; 26: 2713–2722.
47. Roberts SK *et al*. Modulation of uptake of heme by rat small intestinal mucosa in iron deficiency. *Am J Physiol* 1993; 265: G712–G718.
48. Worthington MT *et al*. Characterization of a human plasma membrane heme transporter in intestinal and hepatocyte cell lines. *Am J Physiol Gastrointest Liver Physiol* 2001; 280: 1172–1177.
49. Uc A *et al*. Heme transport exhibits polarity in caco-2 cells: evidence for an active and membrane protein-mediated process. *Am J Physiol Gastrointest Liver Physiol* 2004; 287: G1150–G1157.
50. Conroy Sun RSMZ. Folic acid-peg conjugated superparamagnetic nanoparticles for targeted cellular uptake and detection by MRI. *J Biomed Mater Res A* 2006; 78A: 550–557.
51. Florence AT *et al*. Factors affecting the oral uptake and translocation of polystyrene nanoparticles: histological and analytical evidence. *J Drug Target* 1995; 3: 65–70.